Proceedings of the 5th International Conference on Civil Engineering for Sustainable Development (ICCESD 2020), 7~9 February 2020, KUET, Khulna, Bangladesh (ISBN-978-984-34-8764-3)

PARAMETRIC SENSITIVITY IN LARGE DEFORMATION ANALYSIS BY SMOOTHED PARTICLE HYDRODYNAMICS (SPH)

Nafisa Tabassum*[1,2], Md. Aftabur Rahman[2] and Mohammed Russedul Islam[3]

[1]Graduate Student (M.Sc Engg. Candidate), Chittagong University of Engineering & Technology, Chattogram-4349, Bangladesh, email: nafisa_t@cuet.ac.bd
[2]Faculty, Department of Civil Engineering, Chittagong University of Engineering & Technology, Chattogram-4349, Bangladesh, email: maftabur@cuet.ac.bd
[3]Faculty, Department of Civil Engineering, Military Institute of Science & Technology, Mirpur Cantonment, Dhaka-1216, Bangladesh, email: ce_russel@yahoo.com

***Corresponding Author**

ABSTRACT

Handling of large deformation with traditional grid-based method suffers mesh distortion and in the extreme case, blow up of the problem domain can occur. To address this, Particle-based approach is the rational way to simulate the behavior of large deformation. Among several Particle-based methods, Smoothed Particle Hydrodynamics (SPH) is proven to be an effective mesh-free method owing to its true particle nature. The application of SPH in the diverse field of engineering, to be specific large deformation analysis of geomaterials is justified by many researchers. However, the sensitivity of parameters often lead to unphysical outcomes and provide an ambiguous response to the problem statement. Notably, the effect of particle spacing, smoothing lengths, kernel functions, constitutive laws are critically important. Moreover, some additional treatments are also necessary to stabilize the numerical simulation. Therefore, highlighting this problem, an attempt is made to quantitatively evaluate the effect of different sensitive parameters on the response of large deformation simulation. A benchmark case of ideal dam break simulation with different configurations and material properties are simulated and their responses are critically discussed.

Keywords: *Large deformation, Mesh-free method, Smoothed particle hydrodynamics, Sensitivity, Parameters.*

1. INTRODUCTION

The limitation of handling large deformation in traditional Finite Element Method (FEM) takes Particle Methods under the spotlight as particle methods are capable of considering large deformation without numerical divergence. From a list of particle methods developed in last few decades, the Smoothed Particle Hydrodynamics (SPH) is proven to be an effective numerical tool. The true nature of particle method and adaptive nature turn this method very effective capturing large deformation despite the limitation of boundary condition. Likewise, some particle methods, no background mesh is required in SPH. This method was firstly developed for solving astrophysical problems in three dimensional open space (Gingold & Monaghan, 1977; Lucy, 1977). Later, it was used in many sectors, such as in both computational solid and fluid mechanics. The earliest applications were on fluid dynamics related fields such as elastic flow (Swegle, 1992), free surface fluid flows and multi-phase flows (Monaghan, 1994, 1997; Monaghan & Kocharyan, 1995; Joseph P. Morris, 2000), turbulence flows (Monaghan, 2002), low-Reynolds number viscous fluid flows (J.P. Morris, Fox, & Zhu, 1997; Takeda, Miyama, & Sekiya, 1994), incompressible fluid flows (Cummins & Rudman, 1999; Shao & Lo, 2003), flow through porous media (J. P. Morris, Zhu, & Fox, 1999; Zhu, Fox, & Morris, 1999). The preceding reviews express the vast application of SPH not limited to hydrodynamics but also free surface and multi-phase flows. The accuracy of those simulations attracted researcher in the field of geotechnical hazard analysis to apply the SPH to see the insight of the related problems. To be specific, the mostly common geotechnical and geological hazard, landslides and debris flows have been simulated in SPH environment by many researchers around the world. Starting from the simplified and idealized viscous model to complicated mixture theory have been formulated and replicate the real scenario in many instances. However, the SPH formulation needs several parameters for numerical stability and assumed based on case studies. The sensitivity of those parameters may influence the outcome and the necessity of critical evaluation of some parameters are due. Specially, for large deformation landslides or debris flows, the sensitivity of numerical parameters are necessary to evaluate the accuracy of the model. No straight forward research works on sensitivity of parameters used in landslides/debris flows have been reported. Considering the fact, an attempt is made to simulate different conditions in SPH environment and sensitivity of different parameters on the response of the model is extracted. The following sections describe in detail the sensitivity analysis of different parameters for modelling large deformation geotechnical hazards.

2. SPH FORMULATIONS

In the SPH method, a set of finite discretized particles represents the entire computational domain. These particles possess certain volume and mass of the material, having physical properties such as velocity, acceleration, density, stress, etc. and move according to the governing conservation equations. The integral representation of a function in the SPH method can be expressed as follows:

$$f(x) = \int_{\Omega} f(x')\,\delta(x - x')\,dx' \tag{1}$$

Where, $f(x)$ represents a function of the three-dimensional position vector x, Ω is the volume of the integral which holds x and $\delta(x - x')$ is the Dirac Delta function. This Dirac Delta function is given by,

$$\delta(x - x') = \begin{cases} 1 & x = x' \\ 0 & x \neq x' \end{cases} \tag{2}$$

If a smoothing function $W(x - x', h)$ is used in place of Dirac Delta function $\delta(x - x')$, the integral representation of $f(x)$ using kernel approximation operator $<>$ is given by,

$$\langle f(x)\rangle = \int_{\Omega} f(x')\,W(x-x',h)\,dx' \tag{3}$$

where, W is the kernel or smoothing function which must satisfy the normalized condition and dirac delta function, h is the smoothing length.

The dimension of the compact support is defined by the smoothing length h and a scaling factor k, where, k=constant, kh specifies the non-zero area (effective) of the smoothing function at point x i.e. radius of the influence domain. This effective area is called the support domain for the smoothing function of point x. Using this compact condition, integration over the entire problem domain is localized as integration over the support domain of the smoothing function.

After some trivial mathematical formulations, for a given particle i, the particle approximation for a function and its spatial derivative at particle i can be expressed as:

$$< f(x_i) >= \sum_{j=1}^{N} \frac{m_j}{\rho_j} f(x_j).W_{ij} \tag{4}$$

where,

$$W_{ij} = W(x_i - x_j, h) = W(|x_i - x_j|, h) \tag{5}$$

and,

$$< \nabla.f(x_i) > = \sum_{j=1}^{N} \frac{m_j}{\rho_j} f(x_j).\nabla_i W_{ij} \tag{6}$$

where,

$$\nabla_i W_{ij} = \frac{x_i - x_j}{r_{ij}} \frac{\partial W_{ij}}{\partial r_{ij}} = \frac{x_{ij}}{r_{ij}} \frac{\partial W_{ij}}{\partial r_{ij}} \tag{7}$$

where, ∇W is the gradient of the smoothing function W; r_{ij} indicates the distance between particle i and j.

Different types of smoothing functions are available for implementation in the SPH literature. Each kernel function has its special feature to use in particular problems. The most widely used one is cubic spline function, proposed by (Monaghan & Lattanzio, 1985), having the following form:

$$W_{ij} = \alpha_d \begin{cases} \frac{2}{3} - q^2 + \frac{1}{2}q^3 & 0 \le q < 1 \\ \frac{1}{6}(2-q)^3 & 1 \le q < 2 \\ 0 & q \ge 2 \end{cases} \tag{8}$$

where α_d= normalization factor, which is $\frac{1}{h}$, $\frac{15}{7\pi h^2}$ and $\frac{3}{2\pi h^3}$ in 1D, 2D and 3D space, $q = \frac{r_{ij}}{h} = \frac{x_i - x_j}{h}$ = the relative distance between particles i and j. $k = 2$ is taken for cubic spline function. The kernel function drops to zero for $|r_{ij}| \ge 2h$, implying that the influence domain in Eq. (8) has a radius of $2h$.

3. GOVERNING EQUATIONS

The governing equations is composed of continuity and motion equations as follows:

$$\frac{D\rho}{Dt} = -\rho \frac{\partial v^{\beta}}{\partial x^{\beta}} \tag{9}$$

$$\frac{Dv^{\alpha}}{Dt} = \frac{1}{\rho}\frac{\partial \sigma^{\alpha\beta}}{\partial x^{\beta}} + f^{\alpha} \tag{10}$$

The total stress tensor $\sigma^{\alpha\beta}$ consists of an isotropic hydrostatic pressure p and a deviatoric shear stress s.

$$\sigma^{\alpha\beta} = -p\delta^{\alpha\beta} + s^{\alpha\beta} \tag{11}$$

Where $\delta^{\alpha\beta}$ is Kronecker's delta.

The fluid hydrostatic pressure p in traditional SPH is calculated based on the fluid density change by an equation of state, assuming a weakly compressible fluid (Monaghan, 1994; J.P. Morris, Fox, & Zhu, 1997). The deviatoric shear stress is considered as purely viscous and depends on the fluid models.

4. POST FAILURE BEHAVIOR OF GEO-MATERIAL

Post failure behavior of soil mass can be considered as fluid flow. Fluids can be classified as Newtonian or non-Newtonian fluid based on their viscosity characteristics. However, the fast moving nature of the detached mass and to consider the accumulation at the depositional end, simplied Newtonian Model is effective and have many applications in real analysis. Keeping this issue, simplified Newtonian model is chosen in the current simulation.

According to the Newtonian fluids, flow behavior of fluids follows a linear relationship between shear stress and strain rate with a zero intercept. The slope of the flow curve is constant and is called the viscosity of the fluid. This relationship is known as Newton's Law of Viscosity.

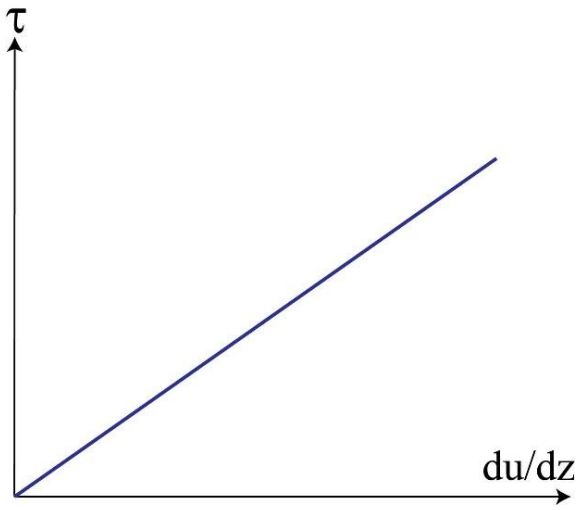

Figure 1: Stress-strain rate relationship of Newtonian model

In 3D analysis , this model is expressed as below:

$$\tau^{\alpha\beta} = \mu\varepsilon^{\alpha\beta} \tag{12}$$

$$\varepsilon^{\alpha\beta} = \frac{\partial v^{\beta}}{\partial x^{\alpha}} + \frac{\partial v^{\alpha}}{\partial x^{\beta}} \tag{13}$$

where, μ is the dynamic viscosity of a fluid, $\tau^{\alpha\beta}$ is the shear stress tensor, $\varepsilon^{\alpha\beta}$ is the strain rate tensor, α and β are Einstein summation index.

5. EVOLUTION OF PRESSURE

Calculation of pressure in SPH method is generally conducted by solving Equation of State (EOS) or Pressure Poisson Equation (PPE). For incompressible SPH (ISPH), the actual EOS will lead to extremely small-time steps, making the entire solution unstable. In this case, pressure is obtained by solving PPE and provide a smoothing pressure distribution especially near the boundary (A. Khayyer, Gotoh, & Shao, 2008; Abbas Khayyer, Gotoh, & Shao, 2009; Ran, Tong, Shao, Fu, & Xu, 2015; Shao & Lo, 2003). However, a comparison was made between standard SPH & ISPH (Shadloo, Zainali, Yildiz, & Suleman, 2012) and compatible results are found for some benchmark tests. Hence, in the current research, pressure was approximated using the widely used EOS (Liu & Liu, 2003), which is given in the following form:

$$p = B\left[\left(\frac{\rho}{\rho_0}\right)^{\gamma} - 1\right] \tag{14}$$

where, ρ_0 is the reference/initial density, ρ is the density at current time step, γ is a dimensionless parameter taken as 7.0 based on literatures, B is the problem dependent parameter and calculated using the following equation.

$$B = \frac{c^2\rho_0}{\gamma} \tag{15}$$

where, c is the speed of sound.

6. USE OF XSPH VARIANT

XSPH technique was first proposed (Monaghan, 1992; Monaghan & Kocharyan, 1995) to correct the velocity term of each particle in SPH problem domain. According to this technique, the particle movement can be obtained as:

$$\frac{dx_i}{dt} = v_i - \varepsilon\sum_{j=1}^{N}\frac{m_j}{\rho_j}v_{ij}W_{ij} \tag{16}$$

where, m_j mass of particle j, ρ_j is density of particle j, $v_{ij}(= v_i - v_j)$ is the velocity difference between particle i and j, W_{ij} is the smoothing function and ε is a constant value ($0 \leq \varepsilon \leq 1.0$). This technique considers the contribution from its neighboring particles. As a result, the particle moves in a velocity closer to the average velocity of its neighboring particles. Most of the applications use ε=0.3 and particles are seen to move more orderly for incompressible flows with XSPH technique (Liu & Liu, 2003). Unphysical penetration between approaching particles can be reduced for compressible flows.

7. BOUNDARY CONDITION

The deficiency of particles near the boundary line often lead to penetration of particles beyond the domain or particle blow up can occur. To get rid of this problem, a suitable boundary condition is needed. There have been several methods developed to model this solid boundary condition. Ghost particles were developed to model the free-slip boundary condition for SPH application to solids (Libersky, Petschek, Carney, Hipp, & Allahdadi, 1993). Virtual particles with repulsive forces were proposed for modelling free-slip boundary conditions of a fluid (Monaghan, 1994). For viscous fluid,

no-slip boundary condition was used (J.P. Morris, Fox, & Zhu, 1997; Takeda, Miyama, & Sekiya, 1994). For SPH application to computational geomechanics, no-slip boundary condition was extended to account for stress boundary conditions (Bui, Fukagawa, Sako, & Ohno, 2008).

8. NUMERICAL MODEL FOR SENSITIVITY ANALYSIS

A 3D model was considered to simulate the flow problems under different conditions. The size of the model is chosen in such way that it represents the real scenario (Rahman & Konagai, 2017). Post flow behavior of the detached mass was analyzed in current research. Therefore, the simulation was started in a dam break fashion by releasing the gate at front of the model instantaneously. Afterward, the failed mass started flowing and normalized run-out and height of the flow process was evaluated. The time history of flow path was considered to be a key criterion to check the influence of different parameters. For the current parametric analysis, the different aspect ratio, viscosity, smoothing length, and xSPH coefficient were critically considered.

9. RESULTS & DISCUSSIONS

An attempt is made in this research to quantitatively evaluate the effect of different sensitive parameters on the response of large deformation simulation. A benchmark case of ideal dam break simulation with different configurations and material properties were simulated and their responses were critically discussed.

At first, a simulation was carried out considering normalized run-out distance with time elapse with varying particle sizes (dx=10mm, 15mm, 20mm) for different aspect ratios (1.0, 0.8 & 0.6).

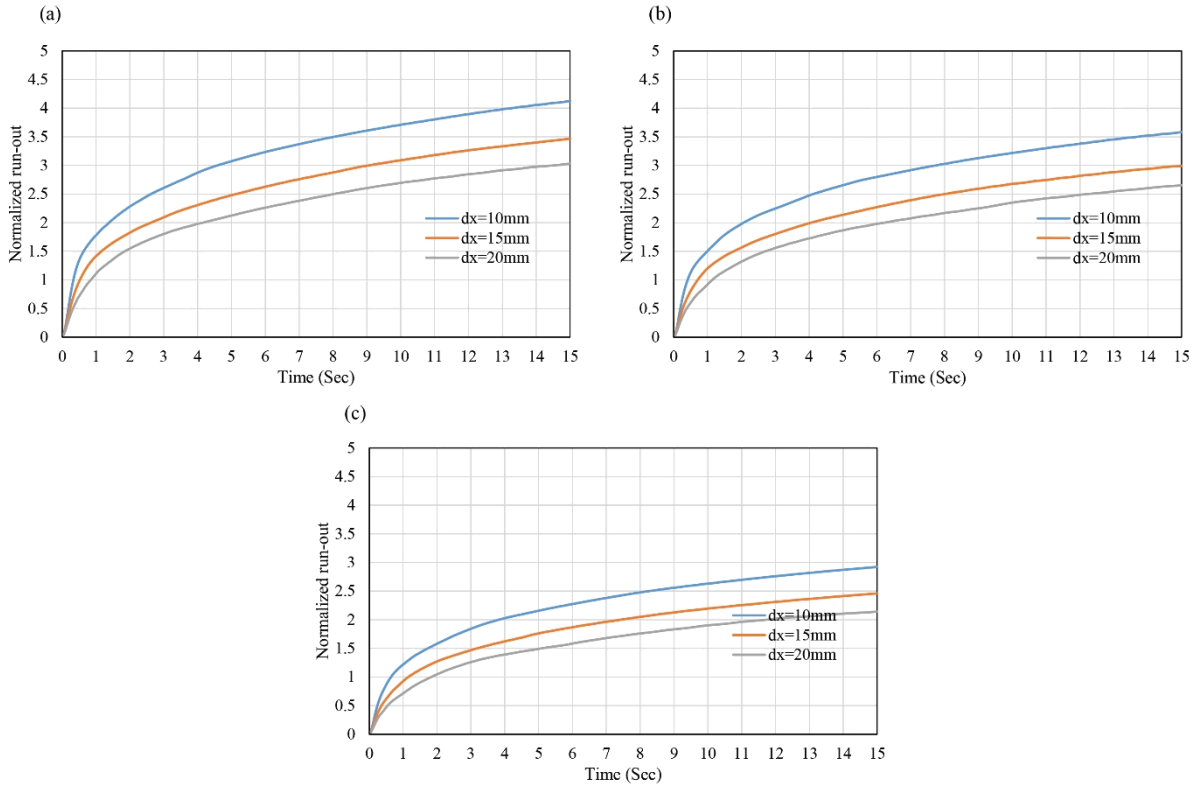

Fig.2: Time-history of normalized surge front; (a) aspect ratio = 1.0, (b) aspect ratio=0.8, (c) aspect ratio=0.6

The time history of normalized surge front for different aspect ratios and different particle sizes are shown in Fig.2. It is seen that normalized run-out distance is found to be increasing with the elapse of time for all cases. Particles with smaller sizes (dx=10mm) show greater runout values than smaller ones. Highest normalized run-out value is found 4.2 for aspect ratio=1.0, whereas this highest value is observed 2.9 for aspect ratio=0.6.

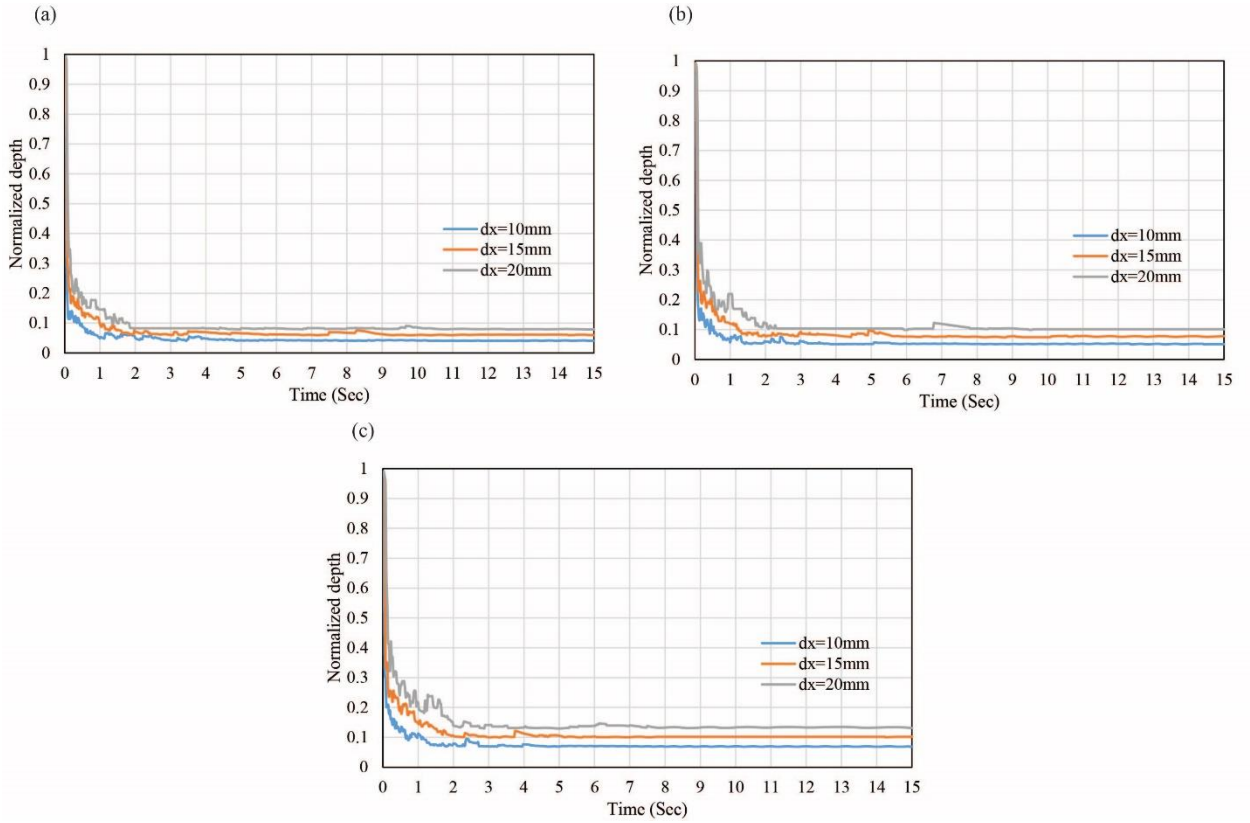

Fig.3: Time-history of normalized front depth; (a) aspect ratio = 1.0, (b) aspect ratio=0.8, (c) aspect ratio=0.6

From the normalized depth vs. time plot shown in Fig.3, it is seen that normalized depth is found decreasing with an increase in time for each aspect ratios. Again, a high fluctuation is observed in the initial 2-3 sec time duration. After that, a quite straight parallel lines are observed for different particle sizes. Again, normalized depth is found greater for larger particle sizes (dx=20mm) than smaller particles ones for three aspect ratio cases (1.0, 0.8 & 0.6).

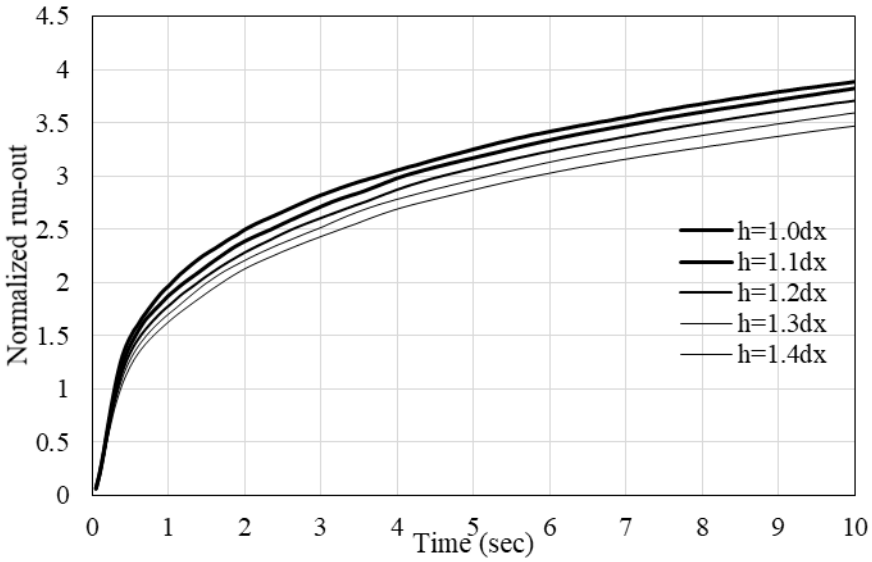

Fig.4: Effect of smoothing length on run-out length in SPH simulation

Later, different smoothing lengths (h=1.0dx, 1.1dx, 1.2dx, 1.3dx, 1.4dx) are taken into consideration and their influences on normalized run-out distance ware also simulated and a graphical representation was plotted (Fig.4). From the plot, normalized run-out was found higher for smaller smoothing lengths (h=1.0dx), whereas it is found lesser for higher smoothing lengths (h=1.4dx).

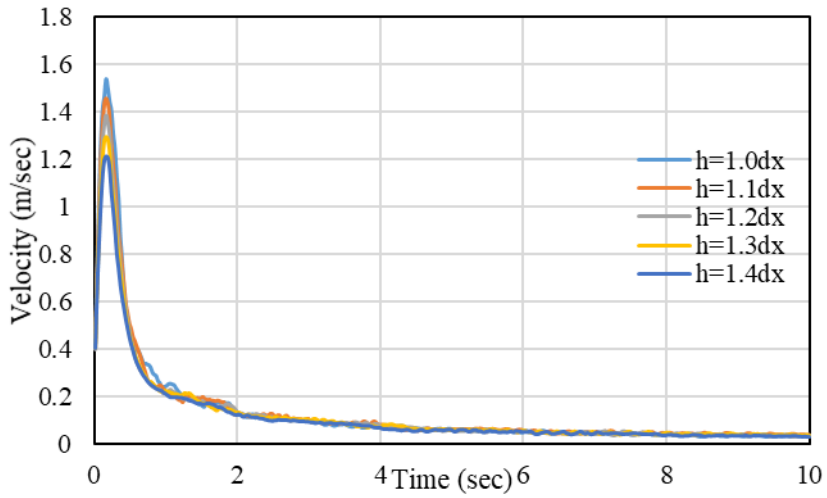

Fig.5: Effect of smoothing length on velocity response in SPH simulation

Next, a simulation was carried out to observe the effect of various smoothing lengths on velocity response of the material. From the graphical plot (Fig.5), it is seen that velocity is found suddenly increasing from a value of 0.4 m/s at time 0 sec to 1.5 m/s at time less than 1 sec (h=1.0dx), followed by a sharp fall to a value less than 0.2 m/s. After 2 sec, velocity profile shows a straight-line pattern with a value less than 0.1 m/s for all smoothing lengths (h = 1.0dx, 1.1dx, 1.2dx, 1.3dx, 1.4dx). But velocity profile depicts variation at the peak curves showing a maximum velocity of 1.5 m/s for smaller smoothing length (h=1.0dx) and a minimum value of 1.2 m/s for larger smoothing length (h=1.4dx).

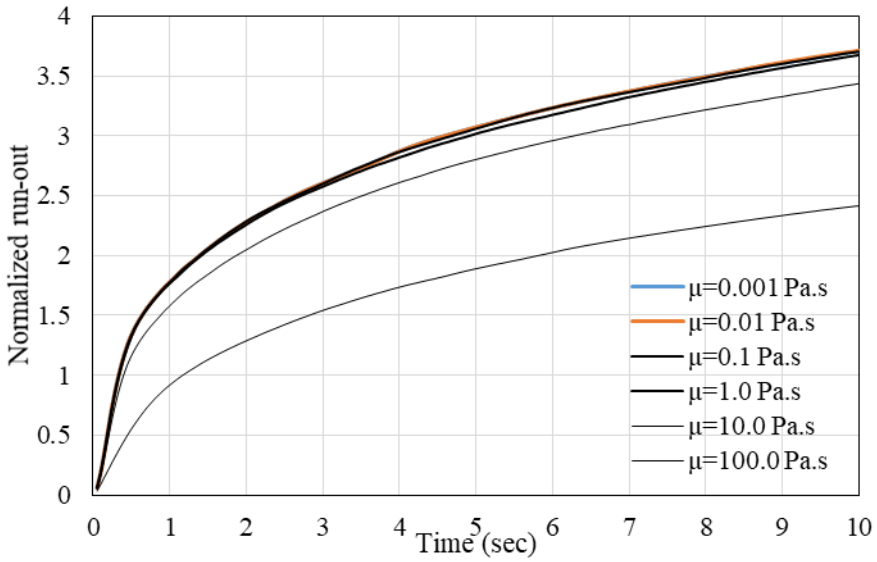

Fig.6: Effect of viscosity on run-out length in SPH simulation

Different viscosity values are taken into consideration to evaluate its effect on run-out distance in our current simulation. Normalized run-out is found decreasing (2.4) with higher viscosity values (100.0 Pa.s), whereas it shows higher value (3.7) for smaller viscosity values less than 1.0 Pa.s (Fig.6).

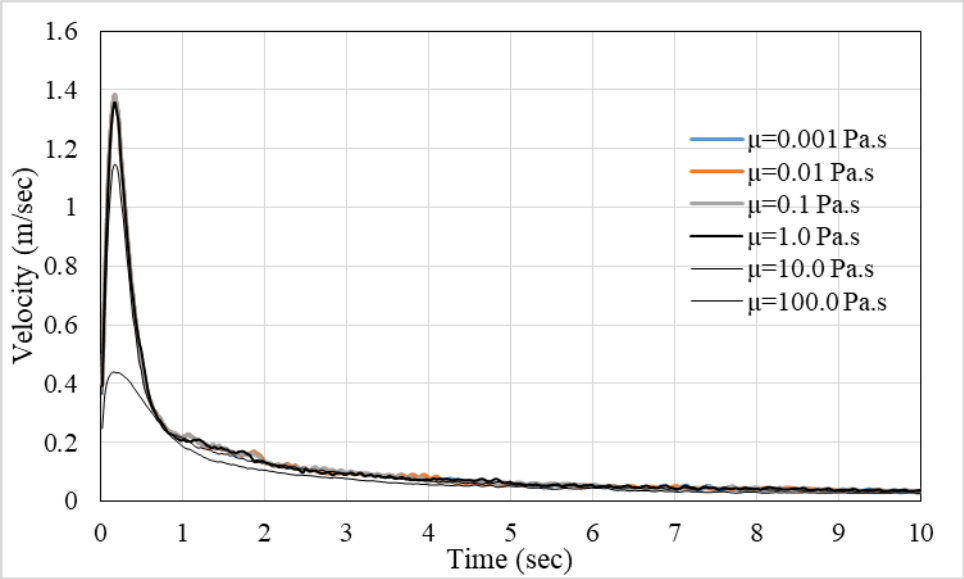

Fig.7: Effect of viscosity on velocity response in SPH simulation

Next, viscosity values on velocity response is simulated. From graphical representation (Fig.7), it is seen that velocity gets its peak almost 1.39 m/s at a time less than 1 sec from 0.25 m/s at time 0 sec. Then velocity profile follows a sudden fall, reaching velocity 0.2 m/s at around 1 sec. After 1 sec, velocity decreases gradually following a straight-line trend for all ranges of viscosity values. Again, less than 1 sec, velocity fluctuates greatly showing 0.43 m/s for higher viscosity (100.0 Pa.s). But peak velocity (1.39 m/s) is observed for smaller viscosity values less than 1.0 Pa.s.

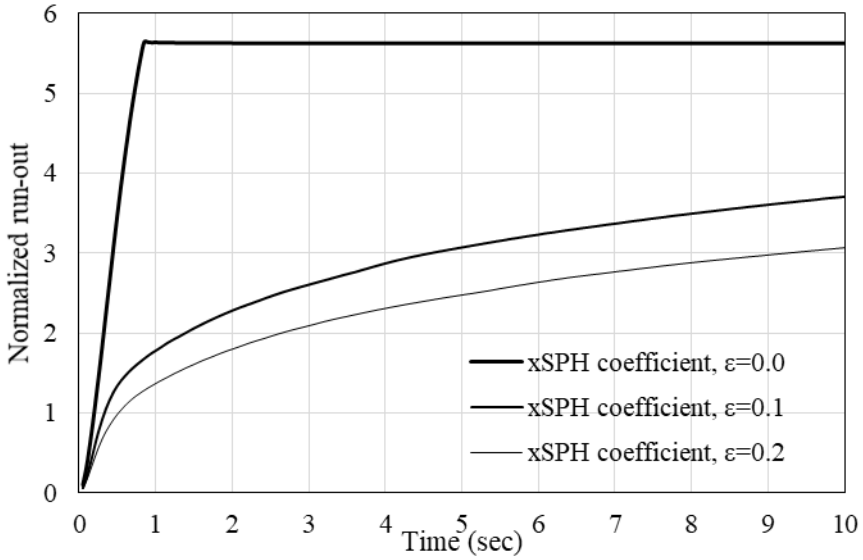

Fig.8: Effect of XSPH coefficient in SPH simulation

XSPH coefficient parameter ε has a great influence on normalized run-out values (Fig.8). For $\varepsilon = 0.0$, run-out distance suddenly increases from 0 to 5.6 up to time 1 sec. After 1 sec, run-out distance follows a constant value 5.6. Again, run-out values are found to increase with a decrease in XSPH coefficient parameter.

10. CONCLUSIONS

The sensitivity of critical parameters was evaluated from series of numerical simulations. A 3D dam break type model, similar to real scale mass considering law of similarity was chosen for numerical analysis. For each cases, simulations were continued to sufficient time to capture the whole scenario. It was found that the particle sizes significantly affect the surge front in SPH environment, which needs to be quantitatively described in real landslide/debris flow simulation by SPH method. The effect of smoothing length and viscosities were not strongly significant and may have freedom in numerical application. In addition, the xSPH coefficient performed quite well in averaging the velocity of particles as the simulation without xSPH coefficient showed divergence for long time simulation. Overall, the sensitivity analysis conducted in this research may provide some useful guidelines for numerical landslide or debris flow modelling in SPH environment. However, the research extent is limited to viscous model, thought there are other methods need to be critically analysed. The future works may highlight the sensitivity of diverse constitutive modelling in SPH environment.

REFERENCES

Bui, H. H., Fukagawa, R., Sako, K., & Ohno, S. (2008). Lagrangian meshfree particles method (SPH) for large deformation and failure flows of geomaterial using elastic-plastic soil constitutive model. *International Journal for Numerical and Analytical Methods in Geomechanics*, *32*(12), 1537–1570. https://doi.org/10.1002/nag

Cummins, S. J., & Rudman, M. (1999). An SPH Projection Method. *Journal of Computational Physics*, *152*(2), 584–607.

Gingold, R. A., & Monaghan, J. J. (1977). Smoothed particle hydrodynamics - Theory and application to non-spherical stars. *Monthly Notices of the Royal Astronomical Society*, *181*, 375–389.

Khayyer, A., Gotoh, H., & Shao, S. D. (2008). Corrected Incompressible SPH method for accurate water-surface tracking in breaking waves. *Coastal Engineering*, *55*(3), 236–250.

https://doi.org/10.1016/j.coastaleng.2007.10.001

Khayyer, Abbas, Gotoh, H., & Shao, S. (2009). Enhanced predictions of wave impact pressure by improved incompressible SPH methods. *Applied Ocean Research*, *31*(2), 111–131. https://doi.org/10.1016/j.apor.2009.06.003

Libersky, L. D., Petschek, A. G., Carney, T. C., Hipp, J. R., & Allahdadi, F. A. (1993). High Strain Lagrangian Hydrodynamics: A Three-Dimensional SPH Code for Dynamic Material Response. *Journal of Computational Physics*, *109*(1), 67–75.

Liu, G. R., & Liu, M. B. (2003). Smoothed Particle Hydrodynamics: A Meshfree Particle Method. *World Scientific Publishing Co. Pte. Ltd*.

Lucy, L. B. (1977). A numerical approach to the testing of the fission hypothesis. *The Astronomical Journal*, *82*(12), 1013–1024. https://doi.org/10.1007/s00769-003-0757-y

Monaghan, J. J. (1992). Smoothed Particle Hydrodynamics. *Annual Review of Astronomy and Astrophysics*, *30*, 543–574. https://doi.org/10.1109/fie.1994.580564

Monaghan, J. J. (1994). Simulating Free Surface Flows With SPH. *Journal of Computational Physics*, *110*(2), 399–406.

Monaghan, J. J. (1997). Implicit SPH Drag and Dusty Gas Dynamics. *Journal of Computational Physics*, *138*(2), 801–820.

Monaghan, J. J. (2002). SPH compressible turbulence. *Monthly Notices of the Royal Astronomical Society*, *335*(3), 843–852. https://doi.org/10.1046/j.1365-8711.2002.05678.x

Monaghan, J. J., & Kocharyan, A. (1995). SPH simulation of multi-phase flow. *Computer Physics Communications*, *87*(1–2), 225–235. https://doi.org/10.1016/0010-4655(94)00174-Z

Monaghan, J. J., & Lattanzio, J. C. (1985). A refined particle method for astrophysical problems. *Astronomy and Astrophysics*, *149*(1), 135–143.

Morris, J. P., Zhu, Y., & Fox, P. J. (1999). Parallel simulations of pore-scale flow through porous media. *Computers and Geotechnics*, *25*(4), 227–246. https://doi.org/10.1016/S0266-352X(99)00026-9

Morris, J.P., Fox, P. J., & Zhu, Y. (1997). Modeling Low Reynolds Number Incompressible Flows Using SPH. *Journal of Computational Physics*, *136*(1), 214–226. https://doi.org/10.1515/polyeng-2016-0102

Morris, Joseph P. (2000). Simulating surface tension with smoothed particle hydrodynamics. *International Journal for Numerical Methods in Fluids*, *33*(3), 333–353. https://doi.org/10.1002/1097-0363(20000615)33:3<333::AID-FLD11>3.0.CO;2-7

Rahman, M. A., & Konagai, K. (2017). Substantiation of debris flow velocity from super-elevation: a numerical approach. *Landslides*, *14*(2), 633–647. https://doi.org/10.1007/s10346-016-0725-3

Ran, Q., Tong, J., Shao, S., Fu, X., & Xu, Y. (2015). Incompressible SPH scour model for movable bed dam break flows. *Advances in Water Resources*, *82*, 39–50. https://doi.org/10.1016/j.advwatres.2015.04.009

Shadloo, M. S., Zainali, A., Yildiz, M., & Suleman, A. (2012). A robust weakly compressible SPH method and its comparison with an incompressible SPH. *International Journal for Numerical Methods in Engineering*, *89*(8), 939–956. https://doi.org/10.1002/nme.3267

Shao, S., & Lo, E. Y. M. (2003). Incompressible SPH method for simulating Newtonian and non-Newtonian flows with a free surface. *Advances in Water Resources*, *26*(7), 787–800. https://doi.org/10.1016/S0309-1708(03)00030-7

Swegle, J. W. (1992). *Report at Sandia National laboratories*.

Takeda, H., Miyama, S. M., & Sekiya, M. (1994). Numerical Simulation of Viscous Flow by Smoothed Particle Hydrodynamics. *Progress of Theoretical Physics*, *92*(5), 939–960. https://doi.org/10.1143/ptp/92.5.939

Zhu, Y. I., Fox, P. J., & Morris, J. P. (1999). A pore-scale numerical model for flow through porous media. *International Journal for Numerical and Analytical Methods in Geomechanics*, *23*(9), 881–904.https://doi.org/10.1002/(SICI)1096-9853(19990810)23:9<881::AID NAG996>3.0.CO;2-K